

# Dicer is required for Sertoli cell function and survival

GWANG-JIN KIM<sup>1,2,#</sup>, INA GEORG<sup>1,2,#</sup>, HARRY SCHERTHAN<sup>3</sup>, MATTHIAS MERKENSCHLAGER<sup>4</sup>,  
FLORIAN GUILLOU<sup>5</sup>, GERD SCHERER<sup>\*,1</sup> and FRANCISCO BARRIONUEVO<sup>\*,1</sup>

<sup>1</sup>Institute of Human Genetics, University of Freiburg, Germany, <sup>2</sup>Faculty for Biology, University of Freiburg, Germany, <sup>3</sup>Bundeswehr Institute of Radiobiology, Munich, and MPI for Molecular Genetics, Berlin, Germany, <sup>4</sup>Lymphocyte Development Group, MRC Clinical Sciences Centre, Imperial College London, UK and <sup>5</sup>UMR 6175, Physiologie de la Reproduction, INRA-CNRS, Université de Tours, Nouzilly, France

**ABSTRACT** Dicer is a key enzyme that processes microRNA precursors into their mature form, enabling them to regulate gene expression. Dicer null mutants die before gastrulation. To study Dicer function in testis development, we crossed mice carrying a conditional Dicer allele with an AMH-Cre transgenic line, thereby inactivating Dicer in Sertoli cells around embryonic day 14.0 (E14.0). Dicer null Sertoli cells show normal embryonic development, and at postnatal day 0 (P0), testis tubules are normal in number and histologically undistinguishable from controls. Subsequently, Dicer-mutant testes show a progressively aberrant development, so that at P6, they contain a reduced number of disorganized testis tubules leading to primary sterility. Apoptosis and prophase I assays reveal a massive wave of apoptosis starting at P3, causing progressive loss of Sertoli cells, but also of germ cells, resulting in drastically reduced testis size. Expression of genes that play crucial roles in testis development, structural integrity and spermatogenesis is downregulated at P0, before morphological changes become apparent, indicating that Dicer-mutant testes are already transcriptionally compromised at this stage. Taken together, the results of this study show that Dicer is required for Sertoli cell function and survival and for spermatogenesis in mice.

**KEY WORDS:** Dicer, miRNAs, testis, spermatogenesis, sterility

## Introduction

Sertoli cells, the somatic, epithelial cells of the testis cords and seminiferous tubules, play central roles during testis development (Wilhelm *et al.* 2007). They are formed shortly after the sex determination stage at embryonic day 11.5 (E11.5), when expression of the testis-determining gene *Sry* in pre-Sertoli cells of the XY gonad causes upregulation of expression of *Sox9*, which initiates a genetic cascade leading to the differentiation of pre-Sertoli into Sertoli cells (Sekido and Lovell-Badge, 2008). During embryonic and fetal development, Sertoli cells are necessary for the formation and integrity of the germ cell-containing testis cords. They are also involved in the degeneration of the Müllerian ducts, the precursors of the female internal genitalia, through the action of the Sertoli cell-secreted factor anti-Müllerian Hormone, AMH, and in the correct differentiation of the interstitial Leydig cells,

which secrete testosterone to promote the differentiation of the Wolffian ducts into the male internal genitalia. Inactivating *Sox9* before E11.5 in XY mice inhibits the formation of Sertoli cells and leads to the development of ovaries in place of testes (Chaboissier *et al.* 2004; Barrionuevo *et al.* 2006). Deletion of Sertoli cell-specific genes *Wt1* (Gao *et al.* 2006) and *Sox9* together with *Sox8* (Barrionuevo *et al.* 2009) at around E14.0, shortly after testis cord formation, causes a wide spectrum of testis abnormalities including loss of testis cord architecture, maintenance of a rudimentary uterus and collapse of the testis resulting in sterility. At puberty, Sertoli cells undergo a process called maturation by which they

*Abbreviations used in this paper:* AMH, anti-Müllerian hormone; En, embryonic day n; EYFP, enhanced yellow fluorescent protein; PLZF, promyelocytic leukemia zinc finger protein; Pn, postnatal day n.

**\*Address correspondence to:** Dr. Francisco Barrionuevo. Institute of Human Genetics, Breisacherstr. 33, D-79106 Freiburg, Germany. Fax: +49-761-270-7041. e-mail: francisco.barrionuevo@uniklinik-freiburg.de or Dr. Gerd Scherer. Institute of Human Genetics, Breisacherstr. 33, D-79106 Freiburg, Germany. Fax: +49-761-270-7041. e-mail: gerd.scherer@uniklinik-freiburg.de **#Note:** These authors contributed equally to this work

**Supplementary Material** for this paper (five additional figures) is available at: <http://dx.doi.org/10.1387/ijdb.092874gk>

Accepted: 1 September 2009. Final author-corrected PDF published online: 18 September 2009.

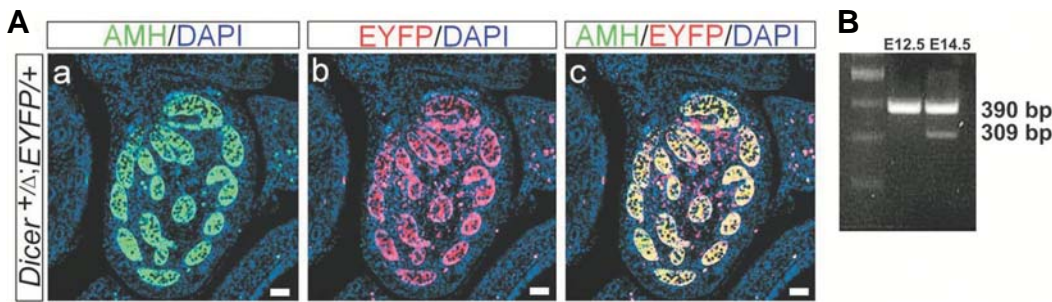


**Fig. 1. Cre activity and *Dicer* inactivation.** (A) Double immunostaining for the Sertoli cell marker AMH (green) (a) and for EYFP (red) (b) on E15.5 *AMH-Cre;Dicer<sup>flox/flox</sup>;EYFP/+* testes revealed co-localization of both signals in all Sertoli cells (overlay) (c). Note that red signals in (b,c) outside testis cords are due to autofluorescence from Leydig cells and blood cells. (B) PCR using genomic DNA of entire *AMH-Cre;Dicer<sup>flox/flox</sup>* testes with primers that give a 390 bp or 309 bp product specific for the undeleted or deleted *Dicer<sup>flox</sup>* allele, respectively, produced a 309 bp fragment at E14.5 but not at E12.5, indicating that the onset of recombination occurs between these stages. Scale bar, 100  $\mu$ m (a-c).

change their morphology and function and establish the blood testis barrier, enabling them to support spermatogenesis. Failure in Sertoli cell maturation causes disorders in spermatogenesis (reviewed in Sharpe *et al.* 2003).

MicroRNAs (miRNAs) are a class of endogenous, noncoding RNAs that negatively regulate protein expression by either mRNA degradation or translational inhibition. The RNase III enzyme Dicer is required for the processing of the 21–22 nucleotides-short miRNAs and small interfering RNAs (siRNAs) from double-stranded RNA precursors (Bartel, 2004). Dicer-generated mature miRNAs are incorporated into the effector RNA-induced silencing complex (RISC) that triggers the destruction of complementary mRNAs or prevents their translation. Several studies have shown testis-specific expression of a number of miRNAs (Ro *et al.* 2007; Yan *et al.* 2007) and of components of the RNA interference machinery (*Drosha*, *Dicer*, *Ago1-4*) (Gonzalez-Gonzalez *et al.* 2008), indicating that they may play a role during testis development. *Dicer*-null mice die at E7.5 (Bernstein *et al.* 2003), preventing the study of the role that *Dicer* may play at later stages of development or in adult tissues. A way to bypass this early lethality consists in the generation of mice harbouring a conditional *Dicer* allele, *Dicer<sup>flox</sup>*, together with a tissue-specifically expressed *Cre* allele. By means of this approach, *Dicer* has been inactivated in a number of discrete tissues (Cobb *et al.* 2005;

Chen *et al.* 2008; De Pietri Tonelli *et al.* 2008; and references therein). In the testis, *Dicer* has recently been conditionally inactivated in primordial germ cells (PGCs), resulting in impaired proliferation of spermatogonia (Hayashi *et al.* 2008).

In the present study, we triggered loss of *Dicer* in Sertoli cells after the sex determination stage by crossing mice carrying a *Dicer<sup>flox</sup>* allele (Cobb *et al.* 2005) with an *AMH-Cre* transgenic mouse line. This line expresses *Cre* under the control of the human *AMH* promoter beginning at around E14.0 (Lécureuil *et al.* 2002). The resulting testes with *Dicer* null Sertoli cells show normal embryonic development, and at P0, testis cords are normal in number and histologically undistinguishable from controls. Subsequently, *Dicer*-mutant testes show a progressively aberrant development, so that at P6, they contain a reduced number of disorganized testis cords where Sertoli and germ cells undergo apoptosis. We also find that spermatogenesis is arrested in the surviving testis cords, explaining why *Dicer* null mice are infertile.

## Results

### Sertoli cell-specific ablation of *Dicer*

To conditionally inactivate *Dicer* in Sertoli cells, we crossed mice with a floxed allele of *Dicer* (*Dicer<sup>flox</sup>*) to mice carrying the Sertoli cell-expressed *AMH-Cre* transgene (Cobb *et al.* 2005; Lécureuil *et al.* 2002). To confirm Sertoli cell-specific ablation of floxed alleles by the *AMH-Cre* transgene, we crossed *AMH-Cre;Dicer<sup>flox/flox</sup>* mice to mice harbouring the Cre reporter allele *R26R-EYFP*. Double immunohistochemistry for AMH, a Sertoli cell marker, and for EYFP on sections of E15.5 *AMH-Cre;Dicer<sup>flox/flox</sup>;EYFP/+* testes revealed Cre-mediated recombination of the *R26R-EYFP* allele in all Sertoli cells (Fig. 1A). The onset of recombination of the *Dicer<sup>flox</sup>* allele in *AMH-Cre;Dicer<sup>flox/flox</sup>*

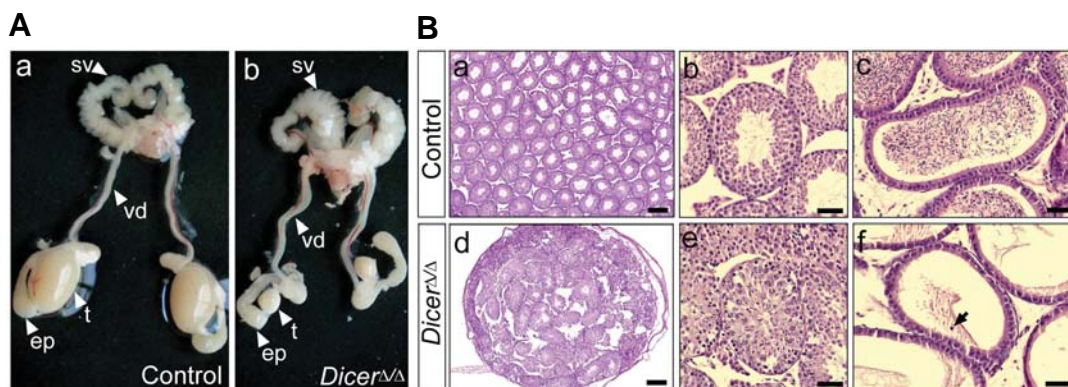


**Fig. 2. Gonadal phenotype of *Dicer<sup>Δ/Δ</sup>* testes at 2 months.** (A) Mutant males had normal appearance of the seminal vesicle, vas deferens and epididymis, but testes were severely reduced in size compared to controls. (B) Hematoxylin/eosin-stained sections. Mutant testes were significantly reduced in size, with testis tubules less densely packed compared to controls (a,d). Higher magnification shows well-developed control tubules full of sperm (b) and mutant testis tubules with a disorganized epithelium and with no lumen and sperm (e). Control epididymides were full of mature sperm (c), whereas mutant epididymides were devoid of mature sperm (f). Occasionally, exfoliated germ cells were visible in mutant epididymides (f, arrow). Ep, epididymis; sv, seminal vesicle; t, testis; vd, vas deferens. Scale bar, 200  $\mu$ m (a,d); 50  $\mu$ m (b,c,e,f).

opened control tubules full of sperm (b) and mutant testis tubules with a disorganized epithelium and with no lumen and sperm (e). Control epididymides were full of mature sperm (c), whereas mutant epididymides were devoid of mature sperm (f). Occasionally, exfoliated germ cells were visible in mutant epididymides (f, arrow). Ep, epididymis; sv, seminal vesicle; t, testis; vd, vas deferens. Scale bar, 200  $\mu$ m (a,d); 50  $\mu$ m (b,c,e,f).

(hereafter designated *Dicer*<sup>ΔΔ</sup>) testes occurs around E14.0, as the 309 bp PCR product specific for the recombined *Dicer*<sup>fllox</sup> allele was undetectable at E12.5, but was clearly detectable at E14.5 (Fig 1B). The 390 bp PCR product diagnostic for the non-recombined *Dicer*<sup>fllox</sup> allele at E14.5 derives from non-Sertoli cells, as DNA from whole testis was used for PCR. The time point of Cre action at around E14.0 is consistent with previous reports in which the *AMH-Cre* transgene has been used for the conditional deletion of other genes in embryonic Sertoli cells (Lécureuil *et al.* 2002; Gao *et al.* 2006; Chang *et al.* 2008; Barrionuevo *et al.* 2009).

### Gonadal phenotype of *Dicer*<sup>ΔΔ</sup> males at 2 months

*Dicer*<sup>ΔΔ</sup> mutant males were viable and showed normal external genitalia but they were sterile as no offspring was obtained when crossed to fertile wildtype females. Analysis of the urogenital tract of *Dicer*<sup>ΔΔ</sup> males at 2 months revealed normal appearance of the seminal vesicles, vasa deferentia and epididymides. In contrast, mutant testes were significantly reduced in size when compared to controls (Fig. 2A). Histologically, mutant testes at 2 months were severely fibrotic, and the few remaining testis tubules were less densely packed compared to the testis tubules in the control littermates (Fig. 2B a,d). Most mutant testis tubules had no lumen and were devoid of mature sperm (Fig. 2Be). Accordingly, no mature sperm was found in the epididymides of mutant males, but occasionally, exfoliated germ cells were visible (Fig. 2Bf, arrow).

### Early postnatal abnormalities of *Dicer*<sup>ΔΔ</sup> testis tubules

To identify the time point at which testis development in *Dicer*<sup>ΔΔ</sup> males derails, we analysed the histology of the mutant gonads during early postnatal development and up to 1 month. At P0, no appreciable difference existed between control and mutant testis tubules (Fig. 3 A,B). But as early as at P3, mutant testis tubules were not as clearly developed as controls, with more interstitial space (Fig. 3 C,D). At P6, mutant testes were smaller than control testes and contained tubules that appeared disorganized and fibrotic (Fig. 3 E-H). The situation was similar at P12, but notably, mutant tubules lacked the central lumen visible at this stage in the control testis tubules (Fig. 3 I,J). At 1 month, mutant testes were much smaller than control testes (Fig. 3 K,L), but appeared more closely packed with testis tubules than at P12 (compare Fig. 3 J with L). Mutant tubules showed a wide range

of anomalies, including tubules with a very reduced size, tubules formed only by Sertoli cells, and tubules lacking the central lumen; no mature sperm was visible in any of these tubules (Fig. 3 M,N).

### Abnormal development of Sertoli cells in *Dicer*<sup>ΔΔ</sup> testes

To trace the development of Sertoli cells in *Dicer*<sup>ΔΔ</sup> testes, we performed IHC for the Sertoli cell marker SOX9. During all stages analysed, Sertoli cells in control testes were located at the periphery of the testis tubules (Fig. 4 A-E). At P0, mutant Sertoli cells were all located at the periphery of the testis tubules (Fig. 4F). At P3, mutant Sertoli cells were mainly located at the periphery, but some cells were also located in the center of the tubules (Fig. 4G, arrow). In contrast, P6 mutant Sertoli cells, which displayed a somewhat less intense and variable SOX9 staining, were mainly located in the center of testis tubules (Fig. 4H), as was also the case for P12 mutant Sertoli cells (Fig. 4I). However, at 1 month, mutant Sertoli cells showed uniform SOX9 staining and were located at the periphery of the testis tubules in the same pattern as control Sertoli cells (Fig. 4 E,J). The same results were obtained by IHC for

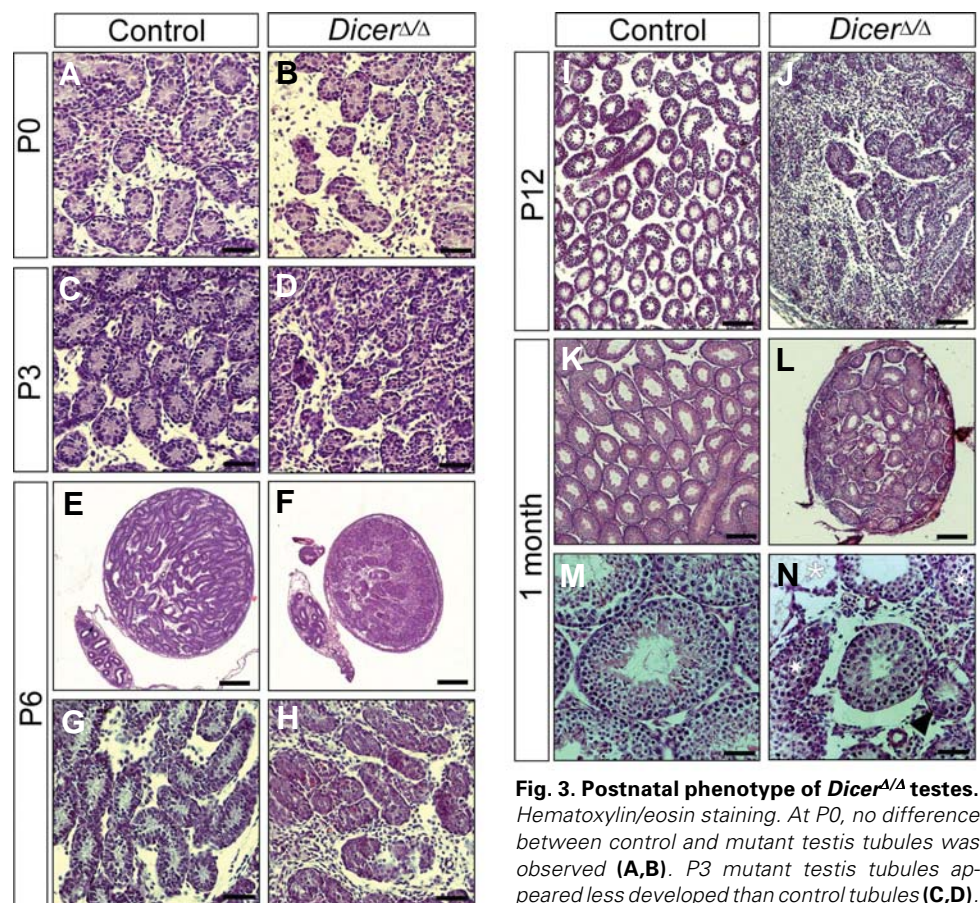


**Fig. 3. Postnatal phenotype of *Dicer*<sup>ΔΔ</sup> testes.** Hematoxylin/eosin staining. At P0, no difference between control and mutant testis tubules was observed (A,B). P3 mutant testis tubules appeared less developed than control tubules (C,D). P6 mutant testes were smaller than controls and displayed a reduction in the number of testis tubules relative to testis size (E,F). High magnification reveals disorganized and fibrotic mutant testis tubules (G,H). A similar situation was found at P12 (I,J). At 1 month, mutant testes were significantly reduced in size, with testis tubules less densely packed compared to controls (K,L). Higher magnification reveals a wide range of anomalies, including tubules with a very reduced size (arrowhead), tubules formed only by Sertoli cells (asterisk), and tubules lacking the central lumen (star) (M,N). Scale bar, 50 μm (A-D, G, H, M, N); 200 μm (E, F, K, L); 100 μm (I, J).

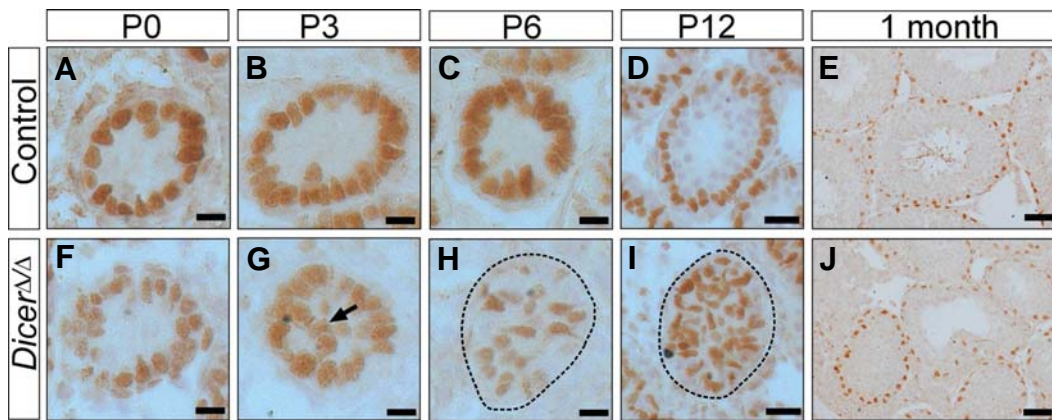


**Fig. 4. Abnormal postnatal development of Sertoli cells in *Dicer* $\Delta/\Delta$  testes.** IHC for the Sertoli cell marker SOX9. At all stages analysed, Sertoli cells were located at the periphery of control testis tubules (A-E). P0 mutant Sertoli cells were located at the periphery (F). P3 mutant Sertoli cells were mainly found at the periphery, but also in the center of the tubules (G, arrow). Mutant Sertoli cells showed non-uniform SOX9 staining and were mainly located in the center of the tubules at P6 (H), and also at P12 (I). At 1 month, mutant Sertoli cells were located at the periphery of the testis tubules in the same pattern as control Sertoli cells (E, J). Scale bar, 10  $\mu$ m (A-C, F-H); 20  $\mu$ m (D, I); 50  $\mu$ m (E, J).

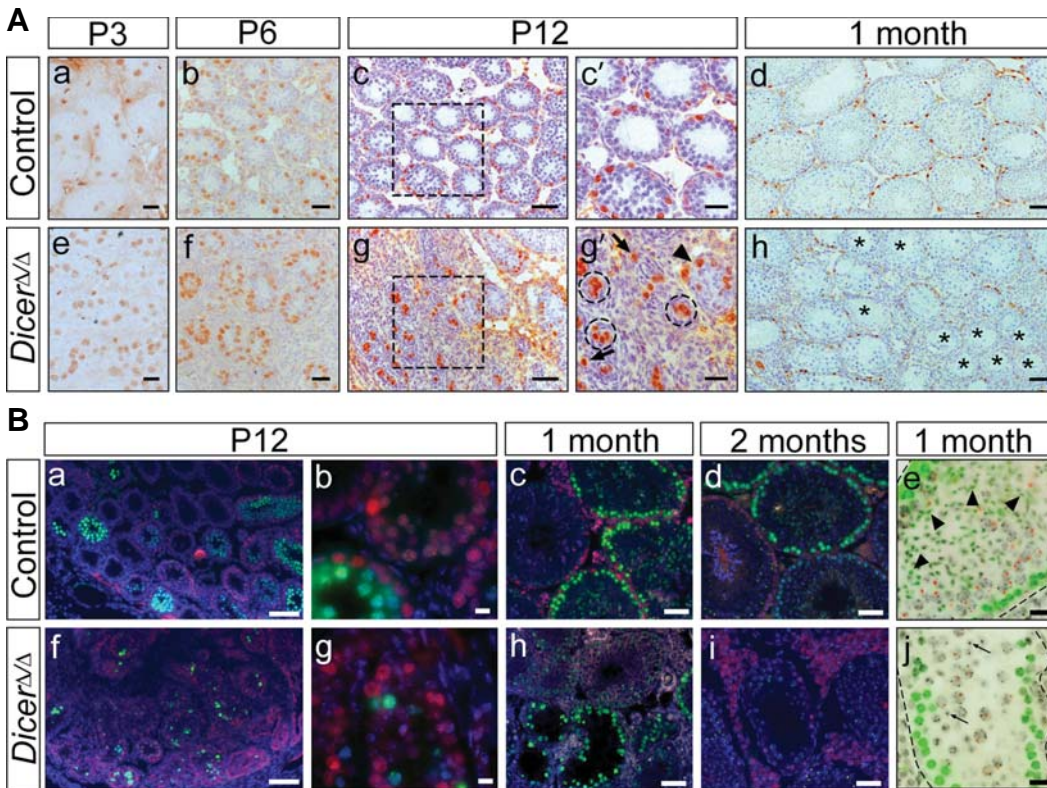


**Fig. 5. Spermatogenesis arrests in *Dicer* $\Delta/\Delta$  testes.** (A) IHC for PLZF.

At P3, PLZF expression was similar in control and mutant testis tubules (a, e). PLZF-positive cells were located at the periphery of control testis tubules at P6, P12 and 1 month (b-d). P6 mutant testis tubules displayed a wildtype pattern of PLZF-positive cells (f). At P12, mutant testes contained tubules with a normal pattern of expression (g', arrowhead), clusters of stained cells surrounded by peritubular myoid cells (g', dashed circles), and single positive cells outside of the tubules (g', arrows). At 1 month, some tubules showed a normal PLZF expression pattern, while other tubules were completely devoid of PLZF-positive cells (h, asterisks). (c', g') Enlargements of the areas boxed in (c, g). (B) Immunofluorescence for  $\gamma$ -H2AX (green), p53BP1 (red), Mre11 (red in e, j) and DNA (DAPI, blue [grey in e, j]) in control (a-e) and *Dicer* $\Delta/\Delta$  testes (f-j). Spermatogonia and Sertoli cells show red nuclear p53BP1 labelling at P12 (a, b, f, g). Synchronous onset of spermatogenesis at P12 as indicated by  $\gamma$ -H2AX-positive leptotene spermatocytes filling the tubules in the wildtype (a, b). A low number of  $\gamma$ -H2AX-positive leptotene spermatocytes marks an asynchronous and delayed onset of spermatogenesis in the P12 *Dicer*-mutant (f, g). This phenotype was also seen after DMC1 staining (Suppl. Fig. S4). One and two month-old control testes showing ordered progression of spermatogenesis with  $\gamma$ -H2AX-bright (green) peritubular leptotene spermatocytes and dimly green stained elongating spermatids in stage IX-X tubules (c, d). Section of a 1 month-old mutant testis showing absence of multi-layered epithelium in several tubules (lower left) that display  $\gamma$ -H2AX-bright leptotene spermatocytes (green) (h). Section of a 2 month-old mutant tubule displaying a few peritubular pachytene spermatocytes whose nuclei feature a  $\gamma$ -H2AX-positive XY body (green dot) while spermatids are absent; large p53BP1-positive (reddish) fibrotic tissue separates the tubules (i). (e, j) Stage IX-X tubule from 1 month-old control and mutant testes displaying peripheral  $\gamma$ -H2AX-bright leptotene spermatocytes (green) and pachytene spermatocytes each with a reddish dot that represents the Mre11 (red)- and  $\gamma$ -H2AX (green)-positive XY body (see Barchi et al. 2005). Dimly  $\gamma$ -H2AX-positive elongated spermatids are present in the control tubule (e, arrowheads), while the mutant tubule contains a few round spermatids only (j, arrows). Note that DAPI staining in (e, j) is colour inverted to gray scale for better visualization. Scale bar, 20  $\mu$ m (Aa, b, e, f); 25  $\mu$ m (Ac', g'); 50  $\mu$ m (Ac, d, g, h); 100  $\mu$ m (Ba, f); 10  $\mu$ m (Bb, g); 50  $\mu$ m (Bc, d, h, i); 20  $\mu$ m (Be, j).

At 1 month, some tubules showed a normal PLZF expression pattern, while other tubules were completely devoid of PLZF-positive cells (h, asterisks). (c', g') Enlargements of the areas boxed in (c, g). (B) Immunofluorescence for  $\gamma$ -H2AX (green), p53BP1 (red), Mre11 (red in e, j) and DNA (DAPI, blue [grey in e, j]) in control (a-e) and *Dicer* $\Delta/\Delta$  testes (f-j). Spermatogonia and Sertoli cells show red nuclear p53BP1 labelling at P12 (a, b, f, g). Synchronous onset of spermatogenesis at P12 as indicated by  $\gamma$ -H2AX-positive leptotene spermatocytes filling the tubules in the wildtype (a, b). A low number of  $\gamma$ -H2AX-positive leptotene spermatocytes marks an asynchronous and delayed onset of spermatogenesis in the P12 *Dicer*-mutant (f, g). This phenotype was also seen after DMC1 staining (Suppl. Fig. S4). One and two month-old control testes showing ordered progression of spermatogenesis with  $\gamma$ -H2AX-bright (green) peritubular leptotene spermatocytes and dimly green stained elongating spermatids in stage IX-X tubules (c, d). Section of a 1 month-old mutant testis showing absence of multi-layered epithelium in several tubules (lower left) that display  $\gamma$ -H2AX-bright leptotene spermatocytes (green) (h). Section of a 2 month-old mutant tubule displaying a few peritubular pachytene spermatocytes whose nuclei feature a  $\gamma$ -H2AX-positive XY body (green dot) while spermatids are absent; large p53BP1-positive (reddish) fibrotic tissue separates the tubules (i). (e, j) Stage IX-X tubule from 1 month-old control and mutant testes displaying peripheral  $\gamma$ -H2AX-bright leptotene spermatocytes (green) and pachytene spermatocytes each with a reddish dot that represents the Mre11 (red)- and  $\gamma$ -H2AX (green)-positive XY body (see Barchi et al. 2005). Dimly  $\gamma$ -H2AX-positive elongated spermatids are present in the control tubule (e, arrowheads), while the mutant tubule contains a few round spermatids only (j, arrows). Note that DAPI staining in (e, j) is colour inverted to gray scale for better visualization. Scale bar, 20  $\mu$ m (Aa, b, e, f); 25  $\mu$ m (Ac', g'); 50  $\mu$ m (Ac, d, g, h); 100  $\mu$ m (Ba, f); 10  $\mu$ m (Bb, g); 50  $\mu$ m (Bc, d, h, i); 20  $\mu$ m (Be, j).

WT1, another Sertoli cell marker (data not shown). That Cre recombinase had successfully acted in all mutant Sertoli cells was demonstrated by IHC for EYFP in 1 month old *Dicer<sup>Δ/Δ</sup>;EYFP/+* mutant testes (Supplementary Fig. S1). Taken together, these results indicate that Sertoli cells follow an aberrant developmental program between P3 and P12 in *Dicer*-mutant testis tubules, but they subsequently manage to organize in the correct manner at the periphery within the few remaining tubules.

### Spermatogenesis arrests in *Dicer<sup>Δ/Δ</sup>* testes

To follow the development of germ cells, we performed IHC for PLZF, a marker for gonocytes at the early stages of testis development, and for spermatogonial stem cells (SSCs) after the onset of meiosis (Buaas *et al.* 2004). At P3, we observed the same pattern of PLZF expression in both control and mutant testis tubules (Fig. 5A a,e). As to be expected for SSCs, PLZF-positive cells were located at the periphery of control testis tubules from P6 onwards (Fig. 5A b-d). PLZF-positive cells were also present at the periphery of mutant testis tubules at P6 (Fig. 5A f). At P12, some mutant tubules showed a normal pattern of expression, but there were also clusters of PLZF-expressing cells surrounded by peritubular myoid cells and single positive cells outside of the tubules (Fig. 5A g,g'). At 1 month, approximately half of the mutant tubules displayed a normal PLZF staining pattern, whereas the remaining tubules were completely devoid of PLZF-positive cells (Fig. 5A h). The number of PLZF-positive cells was determined in six control and six mutant testes, revealing a non-significant two-fold and significant five-fold decrease ( $P < 0.01$ ) at P6 and P12, respectively, per total testis volume in the mutant (Supplementary Fig. S2). As SSCs and undifferentiated spermatogonia in neonatal testis coexpress OCT4 together with PLZF (Filipponi *et al.* 2007), the same stages shown in Fig. 5A were also analyzed by IHC for OCT4. The results were similar to PLZF: mutant tubules

showed normal OCT4 expression pattern up to P6, more mutant tubules than in control were OCT4-negative and some contained OCT4-positive cells away from the periphery at P12, while only very few mutant tubules remained OCT4-positive at 1 month (Supplementary Fig. S3). Altogether, these data indicate that, starting at P6, there is a progressive loss of spermatogonial stem cells in *Dicer<sup>Δ/Δ</sup>* testes.

We next analysed the onset and progression of spermatogenesis in control and mutant testes by immunofluorescence for the DNA repair protein markers p53BP1, Mre11 and  $\gamma$ -H2AX (Fig. 5B). p53BP1 is a marker for non-homologous end-joining DNA repair that is strongly expressed in nuclei of Sertoli cells, intertubular cells and spermatogonia (Ahmed *et al.* 2007). Leptotene and zygotene spermatocyte nuclei strongly express phosphorylated H2AX ( $\gamma$ -H2AX) histones, pachytene spermatocytes show a  $\gamma$ -H2AX- and Mre11-positive XY body (Barchi *et al.* 2005), while elongating spermatids show a diffuse  $\gamma$ -H2AX nuclear signal corresponding to chromatin remodelling and associated DNA double strand break formation that occurs during sperm head condensation (Meyer-Ficca *et al.* 2005). At P12, in control and *Dicer*-mutant testes, Sertoli cells and spermatogonia were positive for p53BP1 (Fig. 5B a,b,f,g). Numerous control tubules displayed characteristic  $\gamma$ -H2AX-positive prophase I stages that filled the tubule lumina (Fig. 5B a,b), while most mutant tubules showed a highly asynchronous onset of spermatogenesis, with only a few  $\gamma$ -H2AX-bright leptotene and zygotene spermatocytes (Fig. 5B f,g). These results were confirmed by the reduced expression of the prophase I-specific DMC1 recombinase in the mutant (Supplementary Fig. S4). At 1 and 2 months, there was normal spermatogenesis in the control (Fig. 5B c-e). *Dicer*-mutant testes at 1 month contained many empty tubules and some stage IX-X tubules that displayed only a peritubular layer of  $\gamma$ -H2AX-positive leptotene spermatocytes, while subsequent stages were missing (Fig. 5B h). Other stage IX-X mutant tubules at 1 month con-

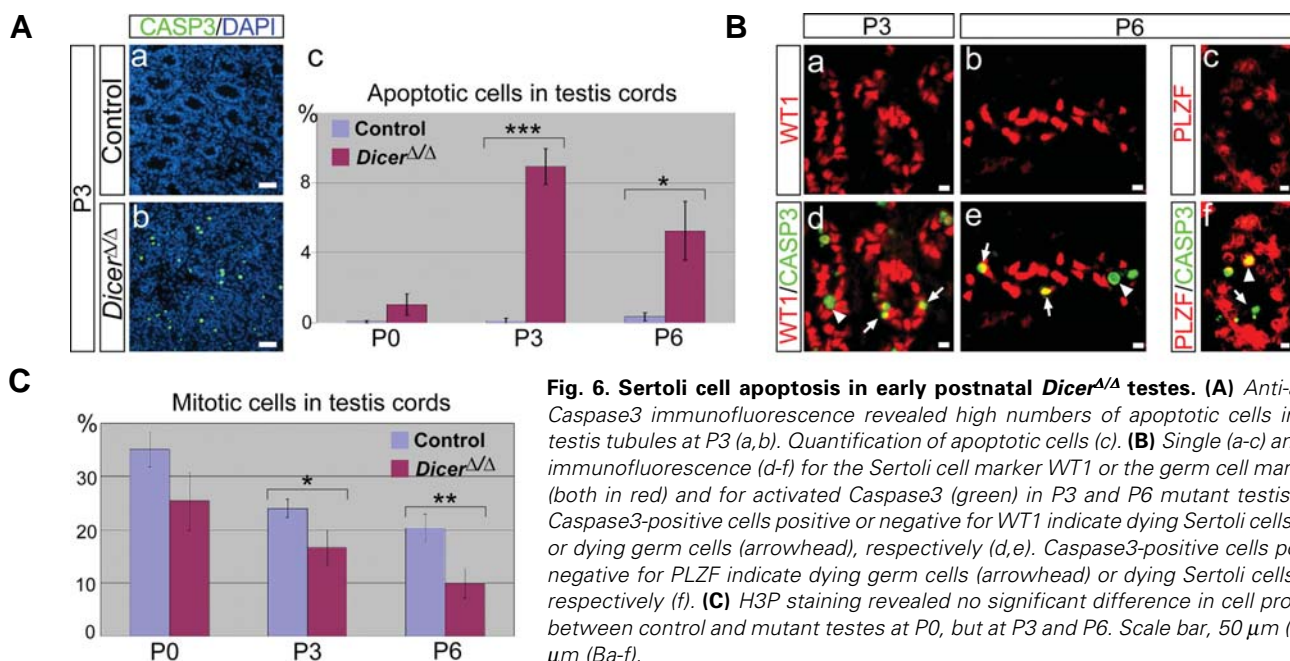


**Fig. 6. Sertoli cell apoptosis in early postnatal *Dicer<sup>Δ/Δ</sup>* testes.** (A) Anti-activated Caspase3 immunofluorescence revealed high numbers of apoptotic cells in mutant testis tubules at P3 (a,b). Quantification of apoptotic cells (c). (B) Single (a-c) and double immunofluorescence (d-f) for the Sertoli cell marker WT1 or the germ cell marker PLZF (both in red) and for activated Caspase3 (green) in P3 and P6 mutant testis tubules. Caspase3-positive cells positive or negative for WT1 indicate dying Sertoli cells (arrows) or dying germ cells (arrowhead), respectively (d,e). Caspase3-positive cells positive or negative for PLZF indicate dying germ cells (arrowhead) or dying Sertoli cells (arrow), respectively (f). (C) H3P staining revealed no significant difference in cell proliferation between control and mutant testes at P0, but at P3 and P6. Scale bar, 50  $\mu$ m (Aa,b); 10  $\mu$ m (Ba-f).

tained spermatocytes and round spermatids (Fig. 5Bj, arrows) but elongating spermatids, as normally seen in wildtype IX-X tubules (Fig. 5Be, arrowheads), were mostly absent. Two month-old mutant testes showed the same phenotype as at 1 month (Fig. 5Bi). One or 2 month-old mutant testes only rarely contained elongating spermatids (Supplementary Fig. S5). Like the wildtype (Barchi *et al.* 2005), mutant pachytene spermatocytes displayed a  $\gamma$ -H2AX and Mre11-positive XY body (Fig. 5Be, j), indicating that sex chromosome pairing and silencing occurred normally in those mutant cells that reached pachytene. Together, these data document an early and progressive defect in spermatogenesis in the mutant testes.

### Sertoli and germ cell apoptosis in early postnatal *Dicer*<sup>ΔΔ</sup> testes

Since *Dicer*<sup>ΔΔ</sup> mutants appear to lose both Sertoli and germ cells, we next examined whether the mutant testis tubules may degenerate via apoptosis. Immunostaining for activated Caspase3 showed a high number of apoptotic cells throughout the mutant testes at P3 (Fig. 6Ab). Counting of apoptotic cells revealed that apoptosis starts after P0, peaks at P3, and declines at P6 (Fig. 6Ac). These results are consistent with the progressive degradation of the mutant testes observed at the histological level. To identify the nature of apoptotic cells, we next performed double immunostaining for WT1, a Sertoli cell marker, and for activated Caspase3. At P3, most Caspase3-positive cells were also positive for WT1 (Fig. 6Bd, arrows), indicating a significant Sertoli cell death at this stage. Occasionally, we also detected a WT1-negative, Caspase3-positive cell within the testis tubules (Fig. 6Bd, arrowhead), indicating that some germ cells are also dying at this stage. The same situation was observed at P6, but at this stage, the Caspase3 signal was found more equally distributed between WT1-positive and -negative cells (Fig. 6Be). Double IHC for the SSC marker PLZF and for activated Caspase3 confirmed that germ cells are indeed dying at P6 (Fig. 6Bf). Identical results were obtained if SOX9 was used as a Sertoli cell marker instead of WT1 (data not shown). When we analyzed proliferation by staining for phospho-histone H3, a marker for prometaphase and metaphase cells in mitosis and meiosis (Hendzel *et al.* 1997), we observed no significant difference between control and mutant testes at P0, but a significant decrease in cell proliferation in the mutant testes at P3 and P6 (Fig. 6C). Therefore, the progressive size difference between control and mutant testes and the eventual loss of testis tubules in mutant mice seems to be caused both by an increase in apoptosis and by a decrease in cell proliferation.

### Altered gene expression in *Dicer*<sup>ΔΔ</sup> testes at the newborn stage

Real-time RT-PCR analyses were performed on testes from newborn mice, a stage where testicular histology of mutants appeared normal. We examined transcript levels of markers playing crucial roles in testis development and differentiation, spermatogenesis, and structural integrity (Table 1). Compared with control testes, we found that transcript levels of several important markers of Sertoli cells, such as *Sox9*, *Sox8*, *Amh*, *Fgf9* and *Dhh*, were significantly downregulated in P0 mutant testes, except for *Wt1*, which was only slightly reduced. We also examined expression levels of genes for Sertoli cell-derived signalling molecules GDNF (glial cell line-derived neurotrophic factor) and

TABLE 1

### REAL-TIME PCR QUANTIFICATION OF GENE EXPRESSION CHANGES IN *DICER*<sup>ΔΔ</sup> MUTANT TESTES AT P0

	<i>Dicer</i> <sup>lox/lox</sup> ; +/+	<i>Dicer</i> <sup>ΔΔ</sup>	
<i>Sox9</i>	1.01±0.06	0.60±0.04	**
<i>Sox8</i>	1.02±0.09	0.36±0.04	***
<i>Amh</i>	1.00±0.01	0.59±0.02	***
<i>Wt1</i>	1.00±0.04	0.86±0.04	*
<i>Fgf9</i>	1.01±0.06	0.55±0.05	***
<i>Dhh</i>	1.01±0.05	0.50±0.04	***
<i>Gdnf</i>	1.00±0.03	0.32±0.02	***
<i>Fgf2</i>	1.03±0.13	0.73±0.04	
<i>Kl</i>	1.01±0.05	0.62±0.04	***
<i>Bmp4</i>	1.03±0.05	0.65±0.03	**
<i>Connexin43</i>	1.00±0.04	0.39±0.02	***
<i>Occludin</i>	1.00±0.05	0.31±0.04	***
<i>Claudin 11</i>	1.01±0.07	0.27±0.04	***

Five pairs of control and mutant testes were used. Data are mean ± s.e.m. (\**P*<0.05; \*\**P*<0.01; \*\*\**P*<0.001).

FGF2, involved in SSC self-renewal and proliferation (Meng *et al.* 2000; Simon *et al.* 2007), and KL (Kit ligand) and BMP4, involved in SSC differentiation (Pellegrini *et al.* 2003, 2008). Whereas expression levels of *Fgf2* were unchanged, *Kl* and *Bmp4* were downregulated by about 40% and *Gdnf* by about 70%. Furthermore, transcript levels of *Connexin43*, which codes for a protein forming gap junctions between Sertoli cells and between Sertoli cells and germ cells, and of *occludin* and *claudin 11*, which encode tight junction proteins involved in the formation of the blood-testis barrier (Mruk and Cheng, 2004), are reduced by a similar degree as the *Gdnf* transcript levels (Table 1). All of this indicates that, in spite of their morphologically normal appearance, P0 mutant testes and Sertoli cells are already transcriptionally compromised.

### Discussion

To assess the requirement of *Dicer* for the development of Sertoli cells and their relation to spermatogenesis, and to overcome the embryonic lethality associated with *Dicer* null mutants, we have deleted a floxed *Dicer* allele using an *AMH-Cre* deleter strain. Inactivation of *Dicer* in Sertoli cells occurred at around E14.0 and subsequently led to a breakdown of spermatogenesis and a severe decrease in the number of testis tubules leading to primary infertility.

Morphologically, no difference between *Dicer*-ablated testes and control testes was apparent at birth. Thereafter, the development of mutant *Dicer* testes deviated from that of controls, showing a phenotype of spermatogenic failure that increased in severity with age. Concurrently, we found an increase in the number of apoptotic cells. The peak in the number of apoptotic cells was detected at P3, just prior to the beginning collapse of mutant testes at P6. Cell death is a common phenomenon associated with *Dicer* conditional knockouts (Chen *et al.* 2008; De Pietri Tonelli *et al.* 2008; and references therein). Additionally, *in vitro* studies have shown that downregulation of *Dicer* results in accelerated apoptosis (Matskevich *et al.* 2008), and that antisense-inhibition of a number of miRNAs increased the level of apoptosis (Cheng *et al.* 2005). *Dicer* is also essential for the formation of the

heterochromatin structure, and its loss results in cell death with the accumulation of abnormal mitotic cells that show premature sister chromatid separation (Fukagawa *et al.* 2004). In the light of these observations, it is conceivable that the increased apoptosis we observed in *Dicer*-deficient Sertoli cells is the consequence either (i) of the downregulation of miRNAs essential for the regulation of the apoptotic pathway, or (ii) of the role of *Dicer* in establishment of differentiation-dependent heterochromatin marks, or (iii) of a combination of both. The question arises as to why significant apoptosis is occurring only at P3 and later, about nine days after the recombination of the *Dicer<sup>flox</sup>* allele. This could be explained by assuming that Sertoli cells change their gene expression profile during their development and that, as a consequence, they may become more dependent on miRNA-mediated regulation than at earlier stages. Indeed, at around puberty (P8-P12), Sertoli cells undergo a process called maturation in which they change their morphology and function to support the first wave of spermatogenesis. Our results could indicate that shortly before this period, Sertoli cells become more dependent on miRNA-mediated control than at earlier stages. A similar situation has been described recently in neurogenic progenitor cells that were unaffected after *Dicer* ablation at the early stage of neurogenesis but underwent apoptosis at later stages (De Pietri Tonelli *et al.* 2008). This is in accordance with the view of Stark and coworkers (Stark *et al.* 2005) that microRNAs confer precision and robustness to developmental gene expression programs, thus ensuring tissue identity and supporting cell-lineage decisions.

Alternatively, the delay in the onset of Sertoli cell death and faulty development may be a consequence of long-term stability of miRNAs such that their levels start to decrease only after a lag phase of several days following *Dicer* inactivation. In fact, a preliminary analysis of all four of the several Sertoli cell-expressed miRNAs described by Ro and coworkers (Ro *et al.* 2007) indicates no significant change in mutant versus control testes at P0 (data not shown). Despite of this, we observed significant downregulation of essentially all Sertoli cell-expressed transcripts analysed already at P0. Thus, loss of *Dicer* function clearly has an early effect on the transcriptional competence of Sertoli cells that precedes morphologically apparent changes. Interestingly, *Wt1* and *Sox9*, which were both downregulated, have previously been inactivated in a conditional manner using the same *AMH-Cre* transgene that we used in this study. In the case of *Wt1*, this resulted in the prenatal disruption of testis cords and progressive loss of Sertoli and germ cells (Gao *et al.* 2006), while in the case of *Sox9*, concomitant inactivation of *Sox8* caused postnatal failure of the differentiation of testis tubules into seminiferous tubules leading to complete primary infertility (Barrionuevo *et al.* 2009). Thus, the phenotype of the *Dicer*-mutants may partially be explained by the reduced expression of *Wt1*, *Sox9* and *Sox8* we observe at P0.

We also studied the expression of genes encoding molecules important for the structural integrity of the sex cords such as proteins involved in formation of Sertoli-Sertoli or Sertoli-germ cell contacts. Occludin and claudins are components of multiprotein complexes that form the tight junctions of mature Sertoli cells that constitute the blood-testis barrier. This barrier is essential for proper spermatogenesis, as males nullizygous for *occludin* or *claudin 11* are sterile (Gow *et al.* 1999; Saitou *et al.* 2000). In

*Dicer*-mutant testes, mRNA levels were reduced by about 70% for *occludin* and *claudin 11*. Of the more than a dozen connexins found in testicular gap junctions, connexin 43 (CX43) is the best studied and is a component of Sertoli-Sertoli and Sertoli-germ cell gap junctions (Decrouy *et al.* 2004). Recently, a Sertoli cell-specific knockout of *Cx43* was shown to prevent the initiation of spermatogenesis (Brehm *et al.* 2007; Sridharan *et al.* 2007). Similar to *occludin* and *claudin 11*, *Cx43* transcript levels were downregulated to about one third of the wildtype level in *Dicer* testes. These changes were all apparent at P0, prior to histologically detectable abnormalities. It thus seems possible that the primary spermatogenic failure displayed by the *Dicer*-mutant testes results in part also from the reduced expression of these three junctional molecules.

Despite the massive apoptosis within the testis tubules beginning at P3, some *Dicer*-mutant testis tubules survived. This allowed us to follow the development of these tubules during spermiogenesis and spermatogenesis. Monitoring the prophase I-specific pattern of p53BP1 and  $\gamma$ -H2AX expression (Meyer Ficca *et al.* 2005; Ahmed *et al.* 2007), as well as sex body formation in pachytene spermatocytes by  $\gamma$ -H2AX and Mre11 expression, we observed tubules where the seminiferous epithelium at stages IX–XI was disrupted beyond the leptotene spermatocyte layer. In tubules with an undisrupted epithelium, chromosome pairing at pachytene was normal as indicated by normal XY-body formation, but spermiogenesis was mostly arrested at the round spermatid stage, with elongated and elongating spermatids seen only rarely in mutant tubules. This indicates that in the majority of mutant tubules, loss of *Dicer* causes a block to the initiation of spermatid chromatin remodeling that occurs at the elongating spermatid steps (McPherson and Longo, 1993; Marcon and Boissonneault, 2004). In addition, the *Dicer*-mutant testes are losing SSCs, which could be a consequence of the downregulation of *Gdnf*, *Kl* and *Bmp4*, which all encode signalling molecules involved in SSC self-renewal and differentiation.

While this work was in progress, a report appeared that described the phenotype of a Sertoli cell-specific *Dicer* ablation that involved the same *AMH-Cre* line used in our study but a different *Dicer-flox* allele (Papaioannou *et al.* 2009). Their data are in agreement with our results including the severe impairment of the prepubertal spermatogenic wave in *Dicer*-mutant testes due to development of defective Sertoli cells that fail to properly support meiosis and spermatogenesis, the massive Sertoli cell and germ cell apoptosis, and the transcriptional downregulation of major regulators of testicular development or spermatogenesis. They also describe numerous spermatogenic defects and progressive testis degeneration and note the almost complete absence of elongating spermatids in mutant tubules. While they observe increased apoptosis starting at P5, we show that this starts already at P3. Surprisingly, they measured increased proliferation of mutant Sertoli cells at P0, P5 and P15, whereas our study revealed a decrease in proliferation of cells in mutant testis tubules at P0, P3 and P6, which is consistent with decrease in cell proliferation frequently observed in other conditional *Dicer* ablation studies (Murchison *et al.* 2005; Hayashi *et al.* 2008; Kobayashi *et al.* 2008). While Papaioannou *et al.* also noticed that mutant Sertoli cells mislocate towards the center of tubules around P5, they did not describe the phenomenon that they later relocate to the tubular periphery at 1 month, expressing SOX9

stronger than they did at P6 (Fig. 4). As the Cre recombinase has recombined the *R26R-EYFPCre* reporter allele in all Sertoli cells of 1 month-old mutant tubules (Supplementary Fig. S1), it can be inferred that *Dicer* is ablated completely in all Sertoli cells in the mutant. Why *Dicer* null Sertoli cells behave in this manner is not clear. Possibly, only those Sertoli cells survive up to 1 month where the loss of *Dicer* had only a transitory effect. Interestingly, Murchison *et al.* (2005) observed after deletion of *Dicer* in embryonic stem cells that some of the mutant cells are able to overcome the initial defect in proliferation and survive ("escapers"), regaining the potential to establish stem cell lines.

In conclusion, our study shows that *Dicer* function in Sertoli cells is important for the regulation of the events that govern a synchronous onset of spermatogenesis and for the maintenance of a multilayered architecture of the seminiferous epithelium essential for spermatid differentiation.

## Materials and Methods

### Mouse crosses

*Dicer<sup>fllox/fllox</sup>* mice (Cobb *et al.* 2005) were bred to *AMH-Cre* mice (Lécureuil *et al.* 2002) on a C57BL/6 background, and the resulting *AMH-Cre;Dicer<sup>fllox/+</sup>* offspring was backcrossed to *Dicer<sup>fllox/fllox</sup>* mice to obtain *AMH-Cre;Dicer<sup>fllox/fllox</sup>* mice. *R26R-EYFPCre* reporter mice (Srinivas *et al.* 2001) were kindly supplied by Frank Constantini. Primers and PCR conditions for genotyping were used as previously described (Lécureuil *et al.* 2002; Kobayashi *et al.* 2008). Primers to detect the 390 bp product diagnostic for the non-recombined *Dicer<sup>fllox</sup>* allele and the 309 bp product diagnostic for the recombined *Dicer<sup>fllox</sup>* allele were 5'-AGTGTAGCCTTAGCCATTTC-3' and 5'-AGTAAATGTGAGCAATAGTCCCAG-3', respectively, and were used together in a single PCR reaction in combination with primer 5'-CTGGTGGCTTGAGGACAAGAC-3'.

### Histologic and immunohistochemical analysis

For histology, embryos and dissected gonads were collected in PBS, fixed in Serra (ethanol:37% formaldehyde:acetic acid, 6:3:1), embedded in paraffin, sectioned to 7  $\mu$ m, and stained with hematoxylin and eosin. Immunostaining was performed using either the Vectastain ABC Kit or the Vector M.O.M. Immunodetection Kit (both from Vector Laboratories) following the manufacturer's guidelines. The following commercial antibodies were used: SOX9 (catalog no. sc-17341, dilution 1:100), AMH (sc-6886, 1:100), and PLZF (sc-21389, 1:75) (all from Santa Cruz, CA); GFP (3999-100, 1:100, BioVision);  $\gamma$ -H2AX (05-636, 1:500, Biomol); p53BP1 (NB 100-304, 1:500, Acris Antibodies); Mre11 (1:200, Novus Biologicals), and WT1 (M3561, clone 6F-H2, 1:150, DAKO). Stained slides were examined with a Zeiss Axioskop 40 microscope. Images were captured by a Zeiss CCD camera. For immunofluorescence, anti-mouse-TRITC (T 7782, 1:200) and anti-rabbit-FITC (F 0382, 1:200) (both from Sigma) and anti-mouse-Cy2 and anti-rabbit-Cy3 antibodies (both from Dianova) were used. Fluorescent signals were recorded using a Zeiss Axioplan 2 fluorescence microscope equipped with the ISIS imaging system (MetaSystems). Sections of control and mutant gonads were always mounted on the same slide. At least three pairs of control and mutant gonads were analysed for each time point.

### Real-time RT-PCR

Total RNA from P0 testes was extracted using the RNeasy Micro kit (Qiagen) including DNase I treatment. RNA integrity was checked with the Agilent 2100 Bioanalyzer (Agilent Technologies) and samples with an RIN above 9.0 were used. Synthesis of cDNA was performed using oligo dT primers and Superscript III reverse transcriptase (Invitrogen). PCR was performed using the QuantiTect SYBR green real-time PCR kit

(Qiagen). Each sample was measured in duplicate in at least two independent experiments.  $C_T$  values of samples were normalized to the corresponding  $C_T$  values of *Gapdh*, and relative expression levels were calculated by the  $\Delta\Delta C_T$  method (Livak and Schmittgen, 2001). Primer pairs used were:

*Bmp4*, 5'-AGGAGGAGGAGGAAGAGCAGAG-3' and 5'-TGAAGAGGAAACGAAAAGCAGA-3';  
*Fgf2*, 5'-CAAACACTACAACCTCAAGCAGAAGA-3' and 5'-CCAGTCGTTCAAAGAAGAAACAC-3';  
*Kl*, 5'-AGTAATAGGAAAGCCGCAAAGG-3' and 5'-CTCCAAAAGCAAAGCCAATTAC-3';

Primer pairs for all other transcripts are published (Barrionuevo *et al.* 2009; and references therein).

### Analysis of cell proliferation and cell death

For cell proliferation, 7  $\mu$ m sections were stained with an anti-phosphohistone H3 antibody (Upstate, Cat 06-570, 1:200), and for detection of apoptotic cells, the anti-Caspase3-active antibody (R&D Systems, Cat AF-835, 1:100) was used. Both primary antibodies were detected using the ABC kit (Vector Laboratories, Burlingame, CA) following the manufacturer's protocol. The slides were counterstained with hematoxylin. For quantification, positive- and negative-staining cells in 30 randomly selected testis tubules per individual were counted. For each time point and genotype, three different animals were examined. To obtain the percentage of positive cells in the tubules, the number of positive cells was set in relation to the total number of cells.

### Statistical Methods

All values are expressed as the mean  $\pm$  s.e.m. Statistical analysis was performed by the Student's *t* test, and results were considered statistically significant at a *P* value < 0.05 (\*), < 0.01 (\*\*), and < 0.001 (\*\*\*)

### Acknowledgements

We thank Christoph Englert for kind gifts of antibodies, Frank Constantini for the *R26R-EYFP Cre* reporter line, Annika Fischer for help in cell counting, and Serge Nef for sharing unpublished information. This work was supported by grants from the Deutsche Forschungsgemeinschaft to G.S. (Sche 194/15-3, GRK1104).

## References

- AHMED EA, VAN DER VAART A, BARTEN A, KAL HB, CHEN J, LOU Z, MINTER-DYKHOUSE K, BARTKOVA J, BARTEK J, DE BOER P, DE ROOIJ DG (2007). Differences in DNA double strand breaks repair in male germ cell types: lessons learned from a differential expression of *Mdc1* and *53BP1*. *DNA Repair* 6: 1243-1254.
- BARCHI M, MAHADEVAIAH S, DI GIACOMO M, BAUDAT F, DE ROOIJ DG, BURGOYNE PS, JASIN M, KEENEY S (2005). Surveillance of different recombination defects in mouse spermatocytes yields distinct responses despite elimination at an identical developmental stage. *Mol Cell Biol* 25: 7203-7215.
- BARRIONUEVO F, BAGHERI-FAMS, KLATTIG J, KISTR, TAKETOMM, ENGLERT C, SCHERER G (2006). Homozygous inactivation of *Sox9* causes complete XY sex reversal in mice. *Biol Reprod* 74: 195-201.
- BARRIONUEVO F, GEORG I, SCHERTHAN H, LÉCUREUIL C, GUILLOU F, WEGNER M, SCHERER G (2009). Testis development after the sex determination stage is independent of *Sox9* but fails in the combined absence of *Sox9* and *Sox8*. *Dev Biol* 327: 301-312.
- BARTEL D. (2004). MicroRNAs: genomics, biogenesis, mechanism and function. *Cell* 116: 281-297.
- BERNSTEIN E, KIM SY, CARMELL MA, MURCHISON EP, ALCORN H, LI MZ, MILLS AA, ELLEDGE SJ, ANDERSON KV, HANNON GJ (2003). *Dicer* is essential for mouse development. *Nat Genet* 35: 215-217.
- BREHM R, ZEILER M, RUTTINGER C, HERDE K, KIBSCHULL M, WINTERHAGER E, WILLECKE K, GUILLOU F, LÉCUREUIL C, STEGER K, KONRAD L, BIERMANN K, FAILING K, BERMANN M (2007). A Sertoli cell-specific knock-

- out of connexin43 prevents initiation of spermatogenesis. *Am J Pathol* 171:19-31.
- BUAAS FW, KIRSH AL, SHARMA M, MCLEAN DJ, MORRIS JL, GRISWOLD MD, DE ROOIJ DG, BRAUN RE (2004). Plzf is required in adult male germ cells for stem cell self-renewal. *Nat Genet* 36: 647-652.
- CHABOISSIER MC, KOBAYASHI A, VIDAL VI, LÜTZKENDORF S, VAN DE KANT HJK, WEGNER M, DE ROOIJ DG, BEHRINGER RR, SCHEDL A (2004). Functional analysis of *Sox8* and *Sox9* during sex determination in the mouse. *Development* 131: 1891-1901.
- CHEN JF, MURCHISON EP, TANG R, CALLIS TE, TATSUGUCHI M, DENG Z, ROJAS M, HAMMOND SM, SCHNEIDER MD, SELZMAN CH, MEISSNER G, PATTERSON C, HANNON GJ, WANG DZ (2008). Targeted deletion of Dicer in the heart leads to dilated cardiomyopathy and heart failure. *Proc Natl Acad Sci USA* 105: 2111-2116.
- CHANG H, GAO F, GUILLOU F, TAKETO MM, HUFF V, BEHRINGER RR (2008). Wt1 negatively regulates  $\beta$ -catenin signaling during testis development. *Development* 135: 1875-1885.
- CHENG AM, BYROM MW, SHELTON J, FORD LP (2005). Antisense inhibition of human miRNAs and indications for an involvement of miRNA in cell growth and apoptosis. *Nucleic Acids Res* 33: 1290-1297.
- COBB BS, NESTEROVA TB, THOMPSON E, HERTWECK A, O'CONNOR E, GODWIN J, WILSON CB, BROCKDORFF N, FISHER AG, SMALE ST, MERKENSCHLAGER M (2005). T cell lineage choice and differentiation in the absence of the RNase III enzyme Dicer. *J Exp Med* 201: 1367-1373.
- DECROUY X, GASC JM, POINTIS G, SEGRETAIN D (2004). Functional characterization of Cx43 based gap junctions during spermatogenesis. *J Cell Physiol* 200: 146-154.
- DE PIETRI TONELLI D, PULVERS JN, HAFFNER C, MURCHISON EP, HANNON GJ, HUTTNER WB (2008). MiRNAs are essential for survival and differentiation of newborn neurons but not for the expansion of neural progenitors during early neurogenesis in the mouse embryonic neocortex. *Development* 135: 3911-3921.
- FILIPPONI D, HOBBS RM, OTTOLENGHI S, ROSSI P, JANNINI EA, PANDOLFI PP, DOLCI S (2007). Repression of kit expression by Plzf in germ cells. *Mol Cell Biol* 27: 6770-6781.
- FUKAGAWA T, NOGAMI M, YOSHIKAWA M, IKENO M, OKAZAKI T, TAKAMI Y, NAKAYAMA T, OSHIMURA M (2004). Dicer is essential for formation of the heterochromatin structure in vertebrate cells. *Nat Cell Biol* 6: 784-791.
- GAO F, MAITI S, ALAM N, ZHANG Z, DENG JM, BEHRINGER RR, LÉCUREUIL C, GUILLOU F, HUFF V (2006). The Wilms tumor gene, *Wt1*, is required for *Sox9* expression and maintenance of tubular architecture in the developing testis. *Proc Natl Acad Sci USA* 103: 11987-11992.
- GONZALEZ-GONZALEZ E, LOPEZ-CASAS PP, DEL MAZO J (2008). The expression patterns of genes involved in the RNAi pathways are tissue-dependent and differ in the germ and somatic cells of mouse testis. *Biochim Biophys Acta* 1779: 306-311.
- GOW A, SOUTHWOOD CM, LI JS, PARIALI M, RIORDAN GP, BRODIE SE, DANIAS J, BRONSTEIN JM, KACHAR B, LAZZARINI RA (1999). CNS myelin and sertoli cell tight junction strands are absent in *Osp/claudin-11* null mice. *Cell* 99: 649-659.
- HAYASHI K, CHUVA DE SOUSA LOPES SM, KANEDA M, TANG F, HAJKOVA P, LAO K, O'CARROLL D, DAS PP, TARAKHOVSKY A, MISHA EA, SURANI MA (2008). MicroRNA biogenesis is required for mouse primordial germ cell development and spermatogenesis. *PLoS One* 3: e1738.
- HENDZEL MJ, WEI Y, MANCINI MA, VAN HOOSER A, RANALLI T, BRINKLEY BR, BAZETT-JONES DP, ALLIS CD (1997). Mitosis-specific phosphorylation of histone H3 initiates primarily within pericentromeric heterochromatin during G2 and spreads in an ordered fashion coincident with mitotic chromosome condensation. *Chromosoma* 106: 348-360.
- KOBAYASHI T, LU J, COBB BS, RODDA SJ, MCMAHON AP, SCHIPANI E, MERKENSCHLAGER M, KRONENBERG HM (2008). Dicer-dependent pathways regulate chondrocyte proliferation and differentiation. *Proc Natl Acad Sci USA* 105: 1949-1954.
- LÉCUREUIL C, FONTAINE I, CREPIEUX P, GUILLOU F (2002). Sertoli and granulosa cell-specific Cre recombinase activity in transgenic mice. *Genesis* 33: 114-118.
- LIVAK KJ, SCHMITTGEN TD (2001). Analysis of relative gene expression data using real-time quantitative PCR and the 2(-Delta Delta C(T)) Method. *Methods* 25: 402-408.
- MARCON L, BOISSONNEAULT G (2004). Transient DNA strand breaks during mouse and human spermiogenesis: new insights in stage specificity and link to chromatin remodeling. *Biol Reprod* 70: 910-918.
- MCPHERSON S, LONGO FJ (1993). Chromatin structure-function alterations during mammalian spermatogenesis: DNA nicking and repair in elongating spermatids. *Eur J Histochem* 37: 109-128.
- MENG X, LINDAHL M, HYVÖNEN ME, PARVINEN M, DE ROOIJ DG, HESS MW, RAATIKAINEN-AHOKAS A, SAINIO K, RAUVALA H, LAKSO M, PICHEL JG, WESTPHAL H, SAARMAM, SARIOLA H (2000). Regulation of cell fate decision of undifferentiated spermatogonia by GDNF. *Science* 287: 1489-1493.
- MEYER-FICCA ML, SCHERTHAN H, BÜRKLE A, MEYER RG (2005). Poly(ADP-ribose)ylation during chromatin remodeling steps in rat spermiogenesis. *Chromosoma* 114: 67-74.
- MRUK DD, CHENG CY (2004). Sertoli-Sertoli and Sertoli-germ cell interactions and their significance in germ cell movement in the seminiferous epithelium during spermatogenesis. *Endocrinol Rev* 25: 747-806.
- MURCHISON EP, PATRIDGE JF, TAM OH, CHELOUFI S, HANNON GJ (2005). Characterization of Dicer deficient murine embryonic stem cells. *Proc Natl Acad Sci USA* 102: 12135-12140.
- PAPAIANOUDOU MD, PITETTI JL, RO S, PARK C, AUBRY F, SCHAAD O, VEJNAR CE, KÜHNE F, DESCOMBES P, ZDOBNOV EM, MCMANUS MT, GUILLOU F, HARFE BD, YAN W, JÉGOU B, NEF S (2009). Sertoli cell Dicer is essential for spermatogenesis in mice. *Dev Biol* 326: 250-259.
- PELLEGRINI M, GRIMALDI P, ROSSI P, GEREMIA R, DOLCI S (2003). Developmental expression of BMP4/ALK3/SMAD5 signaling pathway in the mouse testis: a potential role of BMP4 in spermatogonia differentiation. *J Cell Sci* 116: 3363-3372.
- PELLEGRINI M, FILIPPONI D, GORI M, BARRIOS F, LOLICATO F, GRIMALDI P, ROSSI P, JANNINI EA, GEREMIA R, DOLCI S (2008). ATRA and KL promote differentiation toward the meiotic program of male germ cells. *Cell Cycle* 7: 3878-3888.
- RO S, PARK C, SANDERS KM, MCCARREY JR, YAN W (2007). Cloning and expression profiling of testis-expressed microRNAs. *Dev Biol* 311: 592-602.
- SAITOU M, FURUSE M, SASAKI H, SCHULZKE JD, FROMM M, TAKANO H, NODA T, TSUKITA S (2000). Complex phenotype of mice lacking occludin, a component of tight junction strands. *Mol Biol Cell* 11: 4131-4142.
- SEKIDO R, LOVELL-BADGE R (2008). Sex determination involves synergistic action of SRY and SF1 on a specific *Sox9* enhancer. *Nature* 453: 930-934.
- SHARPE RM, MCKINNELL C, KIVLIN C, FISHER JS (2003). Proliferation and functional maturation of Sertoli cells, and their relevance to disorders of testis function in adulthood. *Reproduction* 125: 769-784.
- SIMON L, EKMAN GC, TYAGI G, HESS RA, MURPHY KM, COOKE PS (2007). Common and distinct factors regulate expression of mRNA for ETV5 and GDNF, Sertoli cell proteins essential for spermatogonial stem cell maintenance. *Exp Cell Res* 313: 3090-3099.
- SRIDHARAN S, SIMON L, MELING DD, CYR DG, GUTSTEIN DE, FISHMAN GI, GUILLOU F, COOKE, PS (2007). Proliferation of adult sertoli cells following conditional knockout of the Gap junctional protein GJA1 (connexin 43) in mice. *Biol Reprod* 76: 804-812.
- SRINIVAS S, WATANABE T, LIN C, WILLIAM CM, TANABE Y, JESSELL TM, COSTANTINI F (2001). Cre reporter strains produced by targeted insertion of *EYFP* and *ECFP* into the *ROSA26* locus. *BMC Dev Biol* 1: 4.
- STARK A, BRENNECKE J, BUSHATIN, RUSSELL RB, COHEN SM (2005). Animal MicroRNAs confer robustness to gene expression and have a significant impact on 3' UTR evolution. *Cell* 123: 1133-1146.
- WILHELM D, PALMER S, KOOPMAN P (2007). Sex determination and gonadal development in mammals. *Physiol Rev* 87: 1-28.
- YAN N, LU Y, SUN H, TAO D, ZHANG S, LIU W, MA Y (2007). A microarray for microRNA profiling in mouse testis tissues. *Reproduction* 134: 73-79.

**Further Related Reading, published previously in the *Int. J. Dev. Biol.***

See Special Issue **Pattern Formation** edited by Michael K. Richardson and Cheng-Ming Chuong at:  
<http://www.ijdb.ehu.es/web/contents.php?vol=53&issue=5-6>

**Gonadal defects in Cited2 -mutant mice indicate a role for SF1 in both testis and ovary differentiation**

Alexander N. Combes, Cassy M. Spiller, Vincent R. Harley, Andrew H. Sinclair, Sally L. Dunwoodie, Dagmar Wilhelm and Peter Koopman  
*Int. J. Dev. Biol.* (2010) 54: 683-689 (doi: 10.1387/ijdb.092920ac)

**The spatio-temporal pattern of testis organogenesis in mammals - insights from the mole**

Francisco D. Carmona, Darío G. Lupiáñez, José-Ezequiel Martín, Miguel Burgos, Rafael Jiménez and Federico Zurita  
*Int. J. Dev. Biol.* (2009) 53: 1035-1044

**Aard is specifically up-regulated in Sertoli cells during mouse testis differentiation**

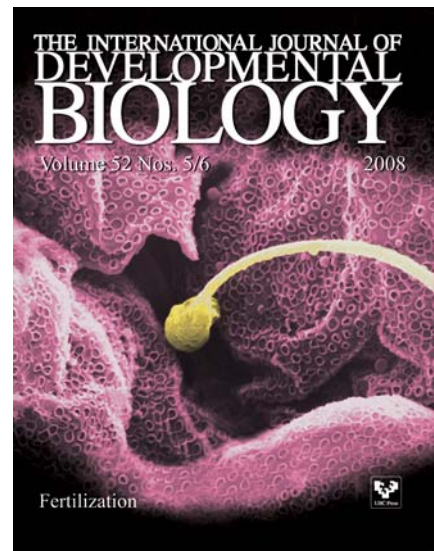
Terje Svingen, Annemiek Beverdam, Pali Verma, Dagmar Wilhelm and Peter Koopman  
*Int. J. Dev. Biol.* (2007) 51: 255-258

**Effects of FGF9 on embryonic Sertoli cell proliferation and testicular cord formation in the mouse**

Louise Willerton, Robert A. Smith, David Russell and Sarah Mackay  
*Int. J. Dev. Biol.* (2004) 48: 637-643

**Abnormal sex-duct development in female moles: the role of anti-Müllerian hormone and testosterone**

Federico Zurita, Francisco J Barrionuevo, Philippe Berta, Esperanza Ortega, Miguel Burgos and Rafael Jiménez  
*Int. J. Dev. Biol.* (2003) 47: 451-458



**5 yr ISI Impact Factor (2008) = 3.271**

